Inorganic Chemistry

Article

pubs.acs.org/IC

Mixed-Valence Heptanuclear Iron Complexes with Ferromagnetic Interaction

Ivan Šalitroš,*[,†] Roman Boča,[†] Radovan Herchel,[‡] Ján Moncol,[†] Ivan Nemec,[‡] Mario Ruben,[§] and Franz Renz[∥]

[†]Institute of Inorganic Chemistry, Faculty of Chemical and Food Technology, Slovak University of Technology, SK-812 37 Bratislava, Slovakia

[‡]Regional Centre of Advanced Technologies and Materials, Department of Inorganic Chemistry, Faculty of Science, Palacký University, 17. Listopadu 12, CZ-77146 Olomouc, Czech Republic

[§]Institute of Nanotechnology, Karlsruhe Institute of Technology, Postfach 3640, D-76021 Karlsruhe, Germany

[∥]Institut für Anorganische Chemie, Leibniz Universität Hannover, Callinstrasse 9, D-30167 Hannover, Germany

Supporting Information

ABSTRACT: Three new Prussian blue analogues, heptanuclear mixed-valence iron complexes of the type $[Fe^{II}(CN)_6\{Fe^{III}(1_{-2H})\}_6]Cl_2{\cdot}nH_2O$, were synthesized and structurally and spectrally characterized, and their magnetic properties were investigated (1_{-2H} corresponds to doubly deprotoned Schiff-base pentadentate ligands **1a**, *N*,*N*′-bis(2-hydroxybenzylidene)-1,5-diamino-3-azapentane, **1b**, *N*,*N*′-bis(3-ethoxy-2-hydroxybenzylidene)-1,7-diamino-4-azaheptane, or **1c**, *N*,*N*′-bis(3-methoxy-2-hydroxybenzylidene)-1,6-diamino-3-azahexane). These compounds were formed by assembling the $[Fe(CN)_6]^{4-}$ building block with mononuclear complexes of the $[Fe(1_{-2H})Cl]$ type. X-ray structure analysis revealed that the complexes adopt a star-like architecture: the Fe(II) ion lies at the very center, and on its octahedral nodes the Fe(III) sites are coordinated in the $Fe^{II}-C{\equiv}N-Fe^{III}$ manner. The Schiff-base pentadentate ligand moiety 1_{-2H} coordinates a single Fe(III) center in two complexes **3b** and **3c**. Ligands $1a_{-2H}$ in the complex cation of **3a** adopt an unusual coordination mode: three donor atoms of the same ligand (one O and two N) coordinate one Fe(III), whereas the remaining N′ and O′ donor atoms coordinate the neighboring Fe(III) center creating the $\{Fe(ON_2)(N'O')N''\}$ chromophore involving two $1a_{-2H}$ ligand moieties. Moreover, three Fe(III) centers are interconnected with three $1a_{-2H}$ ligands in such a manner that two $\{Fe^{III}_3(1a_{-2H})_3\}$ units form two intramolecular rings. Magnetic investigation of the heptanuclear complexes revealed the high-spin state of all six Fe(III) coordination sites ($s = 5/2$), while the very central Fe(II) site is in the low-spin state ($s = 0$). At low temperature, the ferromagnetic exchange interactions stay evident for all three complexes. Mössbauer spectra of compounds **3a** and **3b** revealed a presence of two different doublets for both compounds: the major doublet is related to six Fe(III) high-spin coordination sites and the minor doublet refers to the low-spin very central Fe(II).

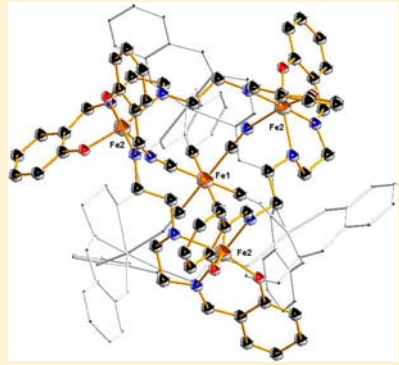

1. INTRODUCTION

Prussian blue analogues (PBAs) have adopted extraordinary importance in the research field of coordination chemistry. The hexadenticity of the $[M(CN)_6]^{m-}$ central bridging anion brings about many opportunities in the syntheses of polynuclear compounds when the ambidentate CN^- ligands allow coordination of peripheral M′ metal ions via the nitrogen donor atoms, M—C≡N—M′. Polynuclearity of such resulting substances is particularly important in the construction of perspective materials with tunable structural, optical, magnetic, and electric properties. Scientific exploration of PBAs began many years ago, and heretofore, thousands of new materials with interesting magnetic properties have already been prepared and characterized; they cover single-molecule magnets,[1,2] spin cross-over systems,[3−5] photoinduced[6−8] and electrochemically[9−11] tuned magnets, or materials with magnetic ordering like ferro- and ferrimagnets.[12−16]

When polydentate ligands are used for coordination to peripheral metal ions M′, a subsequent complexation with the $[M(CN)_6]^{m-}$ anion can lead to a supramolecular architecture where 3D,[17−19] 2D,[20,21] or 1D[22] coordination networks are formed. As an improvement of this synthetic strategy, especially when aiming at the dimensionality of the resulting compounds, the use of the pentadentate N_3O_2 Schiff-base ligands can be mentioned. The remaining sixth coordination site can then be occupied by the chlorido ligands or solvent molecules X, and this labile M′−X bond is easily replaceable by the nitrogen atoms of the cyanido ligands. In such a manner, various 0D polynuclear coordination compounds have already been prepared possessing high-spin properties,[24−28] behaving as

Received: July 20, 2012
Published: November 12, 2012

   dx.doi.org/10.1021/ic3015833 | *Inorg. Chem.* 2012, 51, 12755−12767

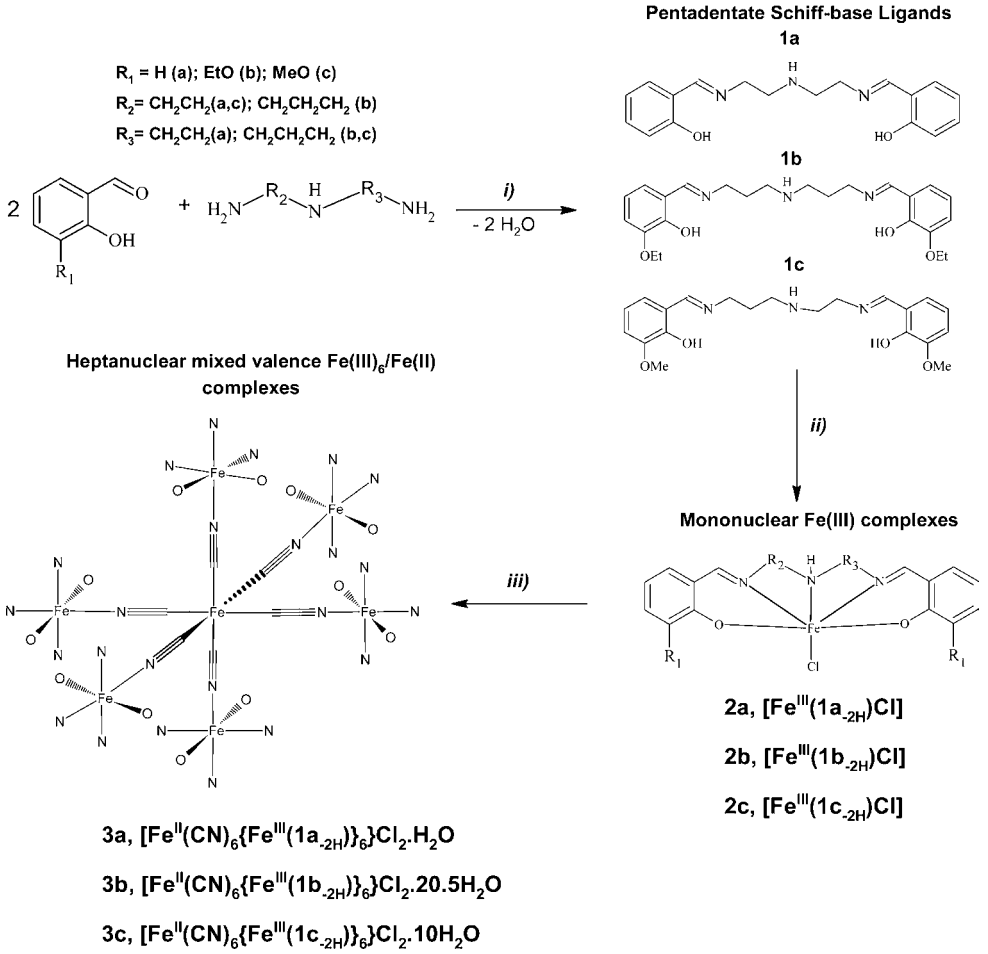

Figure 1. Synthetic route for preparation of heptanuclear compounds **3a**, **3b**, and **3c**; reagents and conditions: (i) CH_3OH, 40 °C, 2 h; (ii) $FeCl_3{\cdot}6H_2O$, $(C_2H_5)_3N$, CH_3OH, 50 °C, 2 h; (iii) $K_4[Fe(CN)]{\cdot}3H_2O$, CH_3CN/CH_3OH, 70 °C, 10 h.

single-molecule magnets,[29] exhibiting ferromagnetism[30−32] or spin cross-over.[33−35]

Herein, we report on the synthesis and spectral, structural, and magnetic characterization of novel heptanuclear mixed-valence Fe(II)−Fe(III)$_6$ complexes adopting a star-like architecture. Their preparation consists of three consecutive steps, i.e., synthesis of N_3O_2−donor Schiff base ligands (**1a**−**c**), coordination with $FeCl_3$ which results in formation of the [Fe(1_{-2H})Cl] mononuclear complexes **2a**−**c** (where 1_{-2H} is a double-deprotonated Schiff-base N_3O_2−donor ligand), and actual synthesis of the polynuclear Fe(II)−Fe(III)$_6$ compounds by coordination of the [Fe(1_{-2H})Cl] species on the hexacyanoferrate anion. Structural investigation of the mononuclear complexes confirmed the expected coordination of one pentadentate ligand with one Fe(III) central atom, where the sixth coordination site is occupied by the Cl^- ligand. The same coordination manner of the Schiff-base ligands was found in two Fe(II)−Fe(III)$_6$ polynuclear systems (**3b** and **3c**). However, the crystal structure of the third heptanuclear complex (**3a**) revealed unusual interconnection of one Fe(III) coordination center by two pentadentate ligands and formation of two intramolecular coordination circles. The magnetic properties (magnetic susceptibility and magnetization) of the prepared compounds have been studied in detail and revealed the high-spin state of the Fe(III) central atoms in mononuclear as well as polynuclear systems.

2. EXPERIMENTAL SECTION

2.1. General. All purchased chemicals were used as received. Methanol, acetonitrile, and diethyl ether were used as solvents without any further purification. Elemental analysis of carbon, hydrogen, and nitrogen was carried out by an automated analyzer (Vario, Micro Cube). IR spectra were measured in KBr pellets in the 4000−400 cm^{-1} region (Magna FTIR 750, Nicolet). Electronic spectra were measured in a Nujol mull (Specord 200, Analytical Jena) in the range of 9000−50 000 cm^{-1}. ^1H and ^{13}C NMR spectra were recorded with the solvent protons as an internal standard (DPX 300, Bruker). Mass spectrometric analytical data were acquired using a matrix-assisted laser desorption/ionization time of flight workstation (MALDI-ToF, Voyager-DE, PRO Bio) and/or electrospray ionization time of flight spectrometer (ESI-ToF, microOTOF-Q II, Bruker).

2.2. Synthesis. Synthesis of heptanuclear compounds **3a**, **3b**, and **3c** consists of three steps (Figure 1): (i) preparation of ligands **1a**, **1b**, and **1c**; (ii) preparation of mononuclear Fe(III) complexes **2a**, **2b**, and **2c** of general formula [Fe(1_{-2H})Cl] (where 1_{-2H} is a deprotoned form of **1a**, **1b**, and **1c** ligands); and (iii) assembling of heptanuclear mixed-valence iron complexes. Mononuclear complex **2d** was prepared in order to explain the crystal structure of heptanuclear compound **3a**.

Ligand ***1a.*** The pentadentate ligand *N*,*N*′-bis(2-hydroxybenzylidene)-1,5-diamino-3-azapentane (**1a**) was prepared by Schiff condensation between 2-hydroxybenzaldehyde (5 mmol) and 1,5-diamino-3-azapentane (2.5 mmol) in a methanol solution (30 cm^3). Both reactants were mixed together at room temperature, and the mixture was stirred at 40 °C for 2 h. After solvent removal the yellow oily material was isolated in more than 95% yield. ^1H NMR (300 MHz, CD_2Cl_2, 25 °C, δ/ppm): 13.32 (s, O*H*), 8.35 (s, 2H, *H*C═N),

dx.doi.org/10.1021/ic3015833 | *Inorg. Chem.* 2012, 51, 12755−12767

7.28 (m, 4H, H_{ar}), 6.88 (m, 4H, H_{ar}), 3.68 (t, 4H, HN−CH_2−CH_2−N═), 2.96 (t, 4H, HN−CH_2−CH_2−N═). ^{13}C NMR (75 MHz, CD_2Cl_2, 25 °C, δ/ppm): 166.08, 161.16, 132.13, 131.41, 118.88, 118.51, 116.74, 59.65, 49.69. MALDI ToF MS (matrix nicotinic acid) m/z: found 312.07 (M^+, 100%); calcd for $C_{18}H_{21}N_3O_2$ (M^+) 311.16. FT IR (KBr; $\overline{\nu}$/cm^{-1}): 3308 (s, O−H), 3255, 3056, 3009, 2895, 2846, 2750, 2660 (w, C−H); 1633, 1582 (s, C═N); 1279 (s, C−O). Anal. Calcd for **1a** $C_{18}H_{21}N_3O_2$ (311.38 g/mol): C, 69.4; N, 13.5; H, 6.80. Found: C, 68.6; N, 13.2; H, 6.66.

Ligand ***1b***. The pentadentate ligand *N*,*N*′-bis(3-ethoxy-2-hydroxybenzylidene)-1,7-diamino-4-azaheptane (**1b**) was prepared by Schiff condensation between 3-ethoxy-2-hydroxybenzaldehyde (5 mmol) and 1,7-diamino-4-azaheptane (2.5 mmol) in a methanol solution (30 cm^3). The reactants combined at room temperature were stirred at 40 °C for 2 h. After solvent removal the yellow oily material resulted in more than 95% yield. ^{1}H NMR (300 MHz, CD_2Cl_2, 25 °C, δ/ppm): 13.70 (s, O*H*), 8.29 (s, 2H, *H*C═N), 6.81 (m, 6H, H_{ar}), 4.01 (q, 4H,OCH_2CH$_3$), 3.61 (t, 4H, HN−CH_2−CH_2−CH_2−N═), 2.65 (t, 4H, HN−CH_2−CH_2−CH_2−N═), 1.80 (t, 4H, HN−CH_2−CH_2−CH_2−N═), 1.38 (t, 6H,OCH$_2$CH_3). ^{13}C NMR (75 MHz, CD_2Cl_2, 25 °C, δ/ppm): 165.08, 152.15, 147.55, 122.84, 118.71, 117.51, 115.36, 64.33, 56.87, 47.20, 31.14, 14.63. MALDI ToF MS (matrix nicotinic acid) m/z: found 426.12 (M^+, 100%); calcd for $C_{24}H_{33}N_3O_4$ (M^+) 427.25. FT IR (KBr; $\overline{\nu}$/cm^{-1}): 3305 (s, O−H), 3057, 2978, 2931, 2850 (w, C−H); 1631, 1584 (s, C═N); 1272, 1251 (s, C−O). Anal. Calcd for **1b** $C_{24}H_{33}N_3O_4$ (427.54 g/mol): C, 67.4; N, 9.87; H, 7.78. Found: C, 67.1; N, 10.0; H, 7.59.

Ligand ***1c***. The pentadentate ligand *N*,*N*′-bis(3-methoxy-2-hydroxybenzylidene)-1,6-diamino-3-azahexane (**1c**) was prepared by Schiff condensation between 3-methoxy-2-hydroxybenzaldehyde (5 mmol) and 1,6-diamino-3-azahexane (2.5 mmol) in a methanol solution (30 cm^3). Both reactants were mixed together at room temperature and then stirred at 40 °C for 2 h. After solvent removal the yellow oily material resulted in more than 95% yield. ^{1}H NMR (300 MHz, CD_2Cl_2, 25 °C, δ/ppm): 13.69 (s, O*H*), 8.35 (s, 1H, *H*C═N),8.30 (s, 1H, *H*C═N) 6.80 (m, 6H, H_{ar}),3.88 (s, 6H,OCH_3), 3,68 (m, 2H, HN−CH_2−CH_2−N═), 3.63 (m, 2H, HN−CH_2−CH_2−CH_2−N═), 2.91 (t, 2H, HN−CH_2−CH_2−N═), 2.71 (t, 2H, HN−CH_2−CH_2−CH_2−N═), 1.83 (t, 2H, HN−CH_2−CH_2−CH_2−N═). ^{13}C NMR (75 MHz, CD_2Cl_2, 25 °C, δ/ppm): 166.01; 165.11, 152.08, 151.91, 148.34, 122.83, 122.77,118.50, 117.58, 117.41, 113.96, 113.84, 56.75, 56.61, 55.81, 54.85, 49.62, 46.79, 30.98. MALDI ToF MS (matrix nicotinic acid) m/z: found 385.97 (M^+, 100%); calcd for $C_{21}H_{27}N_3O_4$ (M^+) 385.46. FT IR (KBr; $\overline{\nu}$/cm^{-1}): 3423 (s, O−H), 3054, 2997, 2967, 2930, 2874, 2830 (w, C−H); 2084 (s, C≡N); 1623, 1598 (s, C═N); 1245, 1223 (s, C−O). Anal. Calcd for **1c** $C_{21}H_{27}N_3O_4$ (385.46 g/mol): C, 65.4; N, 9.87; H, 7.06. Found: C, 64.6; N, 9.91; H, 6.79.

Mononuclear Complexes ***2a*** *(*[Fe(1a$_{-2H}$)Cl]*),* ***2b*** *(*[Fe(1b$_{-2H}$)Cl]·CH_3COCH_3*), and* ***2c*** *(*[Fe(1c$_{-2H}$)Cl]*).* The methanol solution of $FeCl_3$·$6H_2O$ (2.5 mmol, 10 cm^3) was added into the solution of the corresponding Schiff-base ligand **1a**, **1b**, or **1c** (2.5 mmol, 20 cm^3 methanol). The reaction mixture was stirred for 15 min, and then triethylamine (7 mmol) was added. After 2 h of stirring at 50 °C the solution was cooled down (−5 °C); then a dark violet polycrystalline powder was filtered out, washed with cold methanol and diethyl ether, and dried under vacuum. **2a**: ESI ToF MS: $[Fe(1a_{-2H})]^+$ ($C_{18}H_{19}FeN_3O_2$) m/z = 365.08 (calcd m/z = 365.09); $[Fe(1a_{-2H})Cl]Na^+$ ($C_{18}H_{19}ClFeN_3O_2Na$) m/z = 423.04 (calcd m/z = 423.04); $[Fe_2(1a_{-2H})_2Cl]^+$ ($C_{36}H_{38}ClFe_2N_6O_4$) m/z = 823.10 (calcd m/z = 823.09); $[Fe_2(1a_{-2H})_2Cl_2]Na^+$ ($C_{36}H_{38}Cl_2Fe_2N_6O_4Na$) m/z = 823.10 (calcd m/z = 823.09); $[Fe_3(1a_{-2H})_3Cl_3]Na^+$ ($C_{54}H_{57}Cl_3Fe_3N_9O_6Na$) m/z = 1225.15 (calcd m/z = 1225.14). MALDI ToF MS (matrix nicotinic acid) m/z: $[Fe(1a_{-2H})]^+$ ($C_{18}H_{19}FeN_3O_2$) m/z = 365.20 (calcd m/z = 365.09). FT IR (KBr; $\overline{\nu}$/cm^{-1}): 3258 (s, N−H), 3052, 3022, 2977, 2923, 2901, 2869 (w, C−H); 1643, 1628 (s, C═N); 1300 (s, C−O). Anal. Calcd for $[Fe(1a_{-2H})Cl]$ ($C_{18}H_{19}N_3O_2FeCl$; 400.66 g/mol): C, 53.9; N, 10.5; H, 4.78. Found: C, 52.9; N, 10.2; H, 4.69. Yield: 0.82 g (90%). **2b**: ESI ToF MS: $[Fe(1b_{-2H})]^+$ ($C_{24}H_{31}FeN_3O_4$) m/z = 481.16 (calcd m/z = 481.17); $[Fe(1a_{-2H})Cl]Na^+$ ($C_{24}H_{31}FeN_3O_4ClNa$) m/z = 539.21 (calcd m/z = 539.12). MALDI ToF MS (matrix, nicotinic acid) m/z: $[Fe(1b_{-2H})]^+$ ($C_{24}H_{33}N_3O_4Fe$) m/z = 481.12 (calcd m/z = 481.17). FT IR (KBr; $\overline{\nu}$/cm^{-1}): 3248 (s, N−H), 3055, 2971, 2958, 2923, 2896, 2870 (w, C−H); 1704 (C═O); 1614, 1594 (s, C═N); 1241, 1271 (s, C−O). Anal. Calcd for $[Fe(1b_{-2H})Cl]\cdot CH_3COCH_3$ ($C_{27}H_{37}N_3O_5FeCl$; 574.9 g/mol): C, 56.41; H, 6.49; N, 7.31. Found: C, 56.27; H, 6.22; N, 7.24. Yield: 1.12 g (93%). **2c**: ESI ToF MS: $[Fe(1b_{-2H})]^+$ ($C_{21}H_{25}FeN_3O_4$) m/z = 439.11 (calcd m/z = 439.12); $[Fe(1a_{-2H})Cl]Na^+$ ($C_{21}H_{25}FeN_3O_4ClNa$) m/z = 497.16 (calcd m/z = 497.08). MALDI ToF MS (matrix nicotinic acid) m/z: $[Fe(1c_{-2H})]^+$ ($C_{24}H_{33}N_3O_4Fe$) m/z = 438.96 (calcd m/z = 439.12). FT IR (KBr; $\overline{\nu}$/cm^{-1}): 3200 (s, N−H), 3059, 3003, 2953, 2931, 2910, 2860, 2832 (w, C−H); 1636, 1615(s, C═N); 1245, 1217 (s, C−O). Anal. Calcd for $[Fe(1c_{-2H})Cl]$ ($C_{21}H_{25}N_3O_4FeCl$; 474.74 g/mol): C, 53.1; N, 8.85; H, 5.31. Found: C, 52.8; N, 8.83; H, 5.17. Yield: 1.00 g (91%).

Mononuclear Complex ***2d*** *(*[Fe(1a$_{-2H}$)NCS]·CH_3OH*).* A suspension of the complex **2a** (0.2 g, 0.5 mmol, 20 cm^3 methanol/10 cm^3 acetonitrile) was combined with a small excess of KSCN (0.05 g, 0.515 mmol). The reaction mixture was stirred and refluxed for 2 h, and then it was cooled down to room temperature and filtered. The solution was left for a controlled evaporation at room temperature, and within a few days black crystals suitable for structural analysis by X-ray diffraction were filtered off and dried under vacuum. ESI ToF MS: $[Fe(1a_{-2H})]^+$ ($C_{18}H_{19}FeN_3O_2$) m/z = 365.08 (calcd m/z = 365.09); $[Fe(1a_{-2H})NCS]Na^+$ ($C_{19}H_{19}ClFeN_4O_2SK$) m/z = 463.08 (calcd m/z = 463.02); $[Fe_2(1a_{-2H})_2Cl]^+$ ($C_{36}H_{38}ClFe_2N_6O_4$) m/z = 823.10 (calcd m/z = 823.09); $[Fe_2(1a_{-2H})_2(NCS)_2]Na^+$ ($C_{38}H_{38}Cl_2Fe_2N_8O_4SNa$) m/z = 869.11 (calcd m/z = 869.11); $[Fe_3(1a_{-2H})_3(NCS)_3]Na^+$ ($C_{57}H_{57}Cl_3Fe_3N_{12}O_6SNa$) m/z =1292.17 (calcd m/z = 1292.17); $[Fe_4(1a_{-2H})_4(NCS)_4]Na^+$ ($C_{76}H_{76}Cl_4Fe_4N_{16}O_8S_4Na$) m/z =1731.20 (calcd m/z = 1731.20); $[Fe_5(1a_{-2H})_5(NCS)_4]$ ($C_{76}H_{76}Cl_4Fe_4N_{16}O_8S_4Na$) m/z = 2057.32 (calcd m/z = 2057.31). MALDI ToF MS (matrix nicotinic acid) m/z: $[Fe(1a_{-2H})]^+$ ($C_{18}H_{19}FeN_3O_2$) m/z = 365.20 (calcd m/z = 365.09). FT IR (KBr; $\overline{\nu}$/cm^{-1}): 3278 (m, N−H), 3171 (m br, O−H), 3047, 3023 (w, C−H_{arom}); 2974, 2931, 2902, 2867 (w, C−H_{alif}); 2034 (s, NCS); 1639, 1622, 1595 (s, C═N); 1294 (s, C−O). Anal. Calcd for $[Fe(1a_{-2H})NCS]\cdot CH_3OH$ ($C_{20}H_{23}FeN_4O_3S$; 456.34 g/mol): C, 52.8; N, 12.3; H, 5.09. Found: C, 52.6; N, 12.1; H, 5.22. Yield: 0.17 g (74%).

Heptanuclear Mixed-Valence Complexes ***3a***, ***3b***, *and* ***3c***. A 1 mmol amount of the mononuclear complex **2a**, **2b**, or **2c** was dissolved in 70 cm^3 of methanol and heated to 70 °C, Figure 1. Then a stoichiometric amount of $K_4[Fe(CN)_6]\cdot 3H_2O$ (0.167 mmol) dissolved in 5 cm^3 of distilled water was added. The reaction mixture was refluxed for 10 h; then the solution was cooled down to ambient temperature, filtered, and retained for slow evaporation at 5 °C. In a couple of weeks, small dark blue-violet crystals suitable for single-crystal X-ray analysis were collected. **3a**: ESI ToF MS: $[Fe(CN)_6\{Fe(1a_{-2H})\}_6]^{2+}$ ($C_{114}H_{114}Fe_7N_{24}O_{12}$) m/z = 1201.83 (calcd m/z = 1201.59); $[Fe(CN)_6\{Fe(1a_{-2H})\}_6]Cl^+$ ($C_{114}H_{114}Fe_7N_{24}O_{12}Cl$) m/z = 2438.80 (calcd m/z = 2438.64). FT IR (KBr; $\overline{\nu}$/cm^{-1}): 3416 (s, O−H), 2986, 2939, 2906, 2885 (w, C−H); 2067 (s, C≡N), 1620, 1598 (s, C═N); 1295 (s, C−O). Anal. Calcd for $[Fe(CN)_6\{Fe(1a_{-2H})\}_6]Cl_2\cdot H_2O$ ($C_{114}H_{116}Fe_7N_{24}O_{13}Cl_2$; 2492.16 g/mol): C, 54.9; N, 13.5; H, 4.69. Found: C, 54.2; N, 13.1; H, 4.99. Yield: 68%. **3b**: ESI ToF MS: $[Fe(CN)_6\{Fe(1b_{-2H})\}_6]^{2+}$ ($C_{150}H_{186}Fe_7N_{24}O_{12}$) m/z = 1550.13 (calcd m/z = 1549.47). FT IR (KBr; $\overline{\nu}$/cm^{-1}): 3384 (s, O−H), 3052, 2973, 2923, 2867 (w, C−H); 2057 (s, C≡N), 1621, 1595 (s, C═N); 1245, 1222 (s, C−O). Anal. Calcd for $[Fe(CN)_6\{Fe(1b_{-2H})\}_6]Cl_2\cdot 20.5H_2O$ ($C_{150}H_{229}Fe_7N_{24}O_{44.5}Cl_2$; 3540.37 g/mol): C, 51.0; N, 9.52; H, 6.45. Found: C, 50.2; N, 9.43; H, 5.88. Yield 72%. **3c**: ESI ToF MS: $\{[Fe(1c_{-2H})CN]_6Fe\}^{2+}$ ($C_{132}H_{150}Fe_7N_{24}O_{24}$) m/z = 1423.94 (calcd m/z = 1423.83). FT IR (KBr; $\overline{\nu}$/cm^{-1}): 3441 (s, OH), 3054, 2997, 2967, 2874, 2830, (w, C−H), 2084 (s, C≡N), 1622, 1597 (s, C═N); 1245, 1222 (s, C−O). Anal. Calcd for $[Fe(CN)_6\{Fe(1c_{-2H})\}_6]Cl_2\cdot 10H_2O$ ($C_{132}H_{170}Fe_7N_{24}O_{34}Cl_2$; 3098.73 g/mol): C, 51.2; N, 10.8; H, 5.53. Found: C, 51.3; N, 10.5; H, 5.60. Yield: 65%.

2.3. Crystal Structure Determination. Single-crystal X-ray diffraction experiments were conducted using a Gemini R CCD

dx.doi.org/10.1021/ic3015833 | *Inorg. Chem.* 2012, 51, 12755−12767

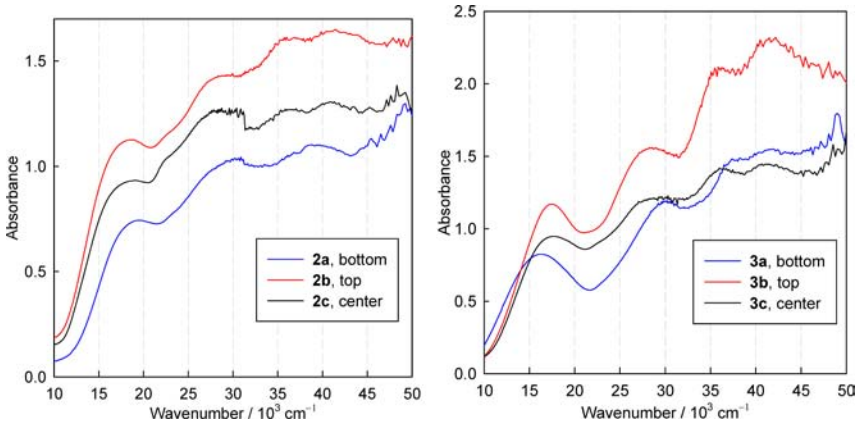

Figure 2. Solid state electronic spectra for mononuclear iron(III) complexes **2a**–**c** (left) and heptanuclear complexes **3a**–**c** (right).

diffractometer (Oxford Diffraction) or Oxford diffractometer Xcalibur2 with the Sapphire CCD detector and fine-focused sealed tube (Mo Kα radiation, λ = 0.71073 Å) source and equipped with an Oxford Cryosystem nitrogen gas-flow apparatus. Data reduction and analytical absorption correction were performed by CrysAlis RED.[36,37] Structures were solved by direct methods using SHELXS-97 or SIR-97 and refined by full-matrix least-squares procedure with the SHELXL-97 program.[38−40] The chloride anions and water molecules in the heptanuclear compounds are strongly disordered in the cavities between the $[Fe(CN)_6\{Fe(L)\}_6]^{2+}$ cations. Attempts in resolving the disorder adequately failed, and therefore, the program PLATON-SQUEEZE was used to remove diffuse electronic density.[40,41] The crystal structure of **3a** contains in the unit cell four voids of 1005 Å^3 containing 45 electrons. This matches the presence of two chloride anions and one water molecule in the empirical formula $[Fe(CN)_6\{Fe(1a_{-2H})\}_6]Cl_2{\cdot}H_2O$. The crystal structure of **3b** contains in the unit cell two voids of 860 Å^3 referring to 239 electrons. This fits to the presence of two chloride anions and 20.5 water molecules in the empirical formula $[Fe(CN)_6\{Fe(1b_{-2H})\}_6]Cl_2{\cdot}20.5H_2O$. The crystal structure of **3c** possesses in the unit cell a single void of 2132 Å^3 containing 299 electrons and three voids of 25 Å^3 containing 14 electrons. This refers to the presence of 2 chloride anions and 10 water molecules in the empirical formula $[Fe(CN)_6\{Fe(1c_{-2H})\}_6]Cl_2{\cdot}10H_2O$.

2.4. Magnetometry. Magnetic measurements were performed using a SQUID magnetometer (MPMS-XL5 and MPMS-XL7, Quantum Design) in the DC and/or RSO mode of detection. In all cases, the temperature dependence of magnetic moment was recorded at 0.1 T as an external magnetic field and the temperature sweeping rate was 1 K/min. The gelatin-made capsules as sample holders were used, and their small diamagnetic signal had a negligible contribution to the overall magnetization, which was dominated by the sample. The diamagnetic corrections to the molar magnetic susceptibilities were applied using Pascal constants.[42]

2.5. Mössbauer Spectroscopy. A conventional Mössbauer spectrometer in the transmission mode with the ^{57}Co/Rh source was utilized. The spectrometer was calibrated to α-Fe at room temperature. All output data are in mm s^{-1}.

3. RESULTS AND DISCUSSION

3.1. Synthesis and Spectroscopic Characterization. The pentadentate N_3O_2-donor Schiff-base ligands **1a** (*N*,*N*′-bis(2-hydroxybenzylidene)-1,5-diamino-3-azapentane), **1b** (*N*,*N*′-bis(3-ethoxy-2-hydroxybenzylidene)-1,7-diamino-4-azaheptane), and **1c** (*N*,*N*′-bis(3-methoxy-2-hydroxybenzylidene)-1,6-diamino-3-azahexane) were prepared in almost quantitative yields by Schiff condensation between a derivative of 2-hydroxybenzaldehyde and an aliphatic triamine. In the consecutive complexation with Fe(III) salts, the mononuclear complexes **2a**, **2b**, and **2c** of general formula $[Fe(1_{-2H})Cl]$ were synthesized (where 1_{-2H} is a double-deprotonated form of the Schiff-base ligand **1a**, **1b**, or **1c**). Single crystals of mononuclear complexes **2b** and **2c** were obtained from the acetone and methanol solution, respectively. Compounds **2b** and **2c** were characterized by single-crystal X-ray diffraction. In order to explain the unusual coordination observed in the case of heptanuclear **3a** compound, the mononuclear complex of formula $[Fe(1a_{-2H})NCS]$ (**2d**) was prepared and structurally characterized.

Reaction between the building blocks $[Fe(1_{-2H})Cl]$ and $[Fe(CN)_6]^{4-}$ resulted in three heptanuclear mixed-valence iron compounds with general formula $[Fe(CN)_6\{Fe(1_{-2H})\}_6]Cl_2{\cdot}nH_2O$. Single crystals suitable for X-ray analysis were obtained by slow evaporation of the mother liquid in a refrigerator. Single-crystal X-ray analysis confirmed formation of heptanuclear dications with formula $[Fe(CN)_6\{Fe(1_{-2H})\}_6]^{2+}$; crystal structures of all three compounds also contain the molecules of crystal water, and the compounds can be described by the following formulas: $[Fe(CN)_6\{Fe(1a_{-2H})\}_6]Cl_2{\cdot}H_2O$ (**3a**), $[Fe(CN)_6\{Fe(1b_{-2H})\}_6]Cl_2{\cdot}20.5H_2O$ (**2b**), and $[Fe(CN)_6\{Fe(1c_{-2H})\}_6]Cl_2{\cdot}10H_2O$ (**3c**) .

The solid state electronic spectra of the herein reported iron complexes were recorded in the Nujol mull as a thin film in transmission mode (Figure 2). The color difference of the dark purple-violet mononuclear and dark blue heptanuclear complexes predestinates different absorption bands in the visible area of the spectra. The visible absorption bands of the mononuclear complexes refer to the phenolato → Fe(III) charge transfer,[43] which is situated at 19 493 cm^{-1} (513 nm) for **2a**, 18 547 cm^{-1} (539 nm) for **2b**, and 19 157 cm^{-1} (522 nm) for **2c**. On the contrary, the visible electronic absorption bands of the heptanuclear Prussian blue analogues are slightly shifted to the lower energies: 16 340 cm^{-1} (612 nm) for **3a**, 17 336 cm^{-1} (577 nm) for **3b**, and 17 638 cm^{-1} (567 nm) for **3c**. It was previously shown that replacement of the chlorido ligand for cyanido nitrogen atoms does not affect the absorption of the Fe(III) coordination centers;[24] therefore, the shift of the electronic absorptions can be attributed to the intervalence charge transfer Fe(II) → Fe(III). The second absorption band of the heptanuclear complexes occurs around 29 000 cm^{-1} (345 nm), and it is analogous to the absorptions of other reported iron Prussian blue analogues of the same structural type.[24,27,35]

Infrared spectroscopy investigation revealed that the heptanuclear Prussian blue analogues **3a**–**c** show many common vibration bands with the corresponding mononuclear complexes **2a**–**c** (see Supporting Information S1), especially in

dx.doi.org/10.1021/ic3015833 | *Inorg. Chem.* 2012, 51, 12755−12767

Table 1. Crystallographic Data for the Mononuclear Complexes

	2b	2c	2d
formula	$C_{27}H_{37}ClFeN_3O_5$	$C_{21}H_{25}ClFeN_3O_4$	$C_{20}H_{23}FeN_4O_3S$
fw/g mol^{-1}	574.90	474.74	455.34
cryst color	dark violet	dark violet	dark violet
temperature/K	100(2)	100(2)	100(2)
wavelength/Å	0.71073	0.71073	0.71073
cryst syst	monoclinic	monoclinic	monoclinic
space group	$P2_1/c$	$P2_1/c$	$P2_1/n$
a/Å	7.5009(2)	9.9099(7)	13.6178(11)
b/Å	13.0058(4)	20.5346(12)	10.1175(8)
c/Å	28.1789(9)	10.9418(8)	14.9168(13)
α/deg	90	90	90
β/deg	93.124(3)	109.064(8)	101.184(8)
γ/deg	90	90	90
V/Å^3	2744.91(14)	2104.5(2)	2016.2(3)
Z, ρ_{calcd}/g cm^{-3}	4, 1.391	4, 1.498	4, 1.500
μ/mm^{-1}	0.688	0.877	0.881
F(000)	1212	988	948
cryst size/mm	0.40 × 0.40 × 0.32	0.35 × 0.28 × 0.22	0.32 × 0.30 × 0.06
final R indices [$I > 2\sigma(I)$]	R_1 = 0.0599	R_1 = 0.0386	R_1 = 0.0654
	wR_2 = 0.1344	wR_2 = 0.0680	wR_2 = 0.1096
R indices (all data)	R_1 = 0.0687	R_1 = 0.0816	R_1 = 0.1089
	wR_2 = 0.1369	wR_2 = 0.0741	wR_2 = 0.1177
GoF on F^2	1.258	0.898	0.967
CCDC ref. no.	838229	838230	838231

the fingerprint region. The major difference lies in the presence of the strong vibration below 2100 cm^{-1}, which is related to the C≡N stretching. In comparison to the uncoordinated $[Fe(CN)_6]^{4-}$ anion, which shows a multiple band centered at 2042 cm^{-1}, the cyanido vibration frequencies are slightly shifted to higher energies. The cyanido bridging ligand vibrations of **3a** and **3c** are unsplit and positioned at 2055 and 2084 cm^{-1}, respectively. However, compound **3b** shows the cyanido vibration split to a 2083 and 2059 cm^{-1} doublet.

3.2. Crystal Structures. *Crystal Structures of Mononuclear Complexes.* Crystal data for the mononuclear Fe(III) complexes **2b–d** are listed in Table 1. Single crystals of complex **2b** were obtained by recrystallization from acetone. The diffraction experiment revealed that the complex consisted of one Fe(III) central atom coordinated with the deprotonated **1b** ligand and one chlorido ligand (Figure 3).

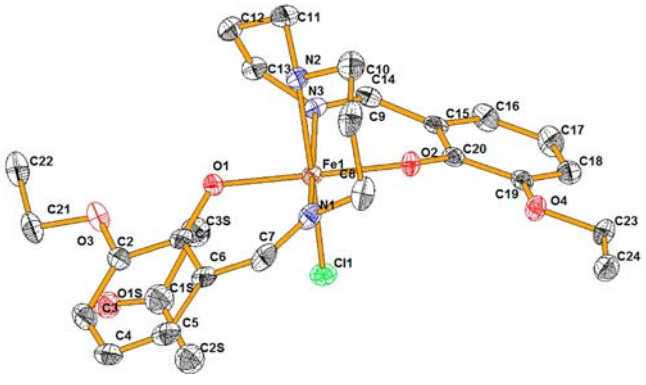

Figure 3. Molecular structure of mononuclear complex **2b** (50% probability level of thermal ellipsoids). Hydrogen atoms are omitted for clarity.

The crystal structure of **2b** contains one nonbonded acetone molecule per formula unit, and four $[Fe(1b_{-2H})Cl]\cdot CH_3COCH_3$ entities are contained in the unit cell. The solvent molecule is connected with the $[Fe(1b_{-2H})Cl]$ moiety by a weak hydrogen bond existing between the O1S oxygen of the acetone molecule and the C14 carbon atom of the imino bond (3.372(6) Å).[44] The $\{FeO_2N_2N'Cl\}$ chromophore forms a distorted tetragonal bipyramid where the Fe–O bond lengths are the shortest (1.957(3) and 1.946(3) Å). The Fe–N(imino) distances are 2.104(4) and 2.097(4) Å, the Fe–N(amino) bond length is 2.234(4) Å, and the longest one is found for the Fe–Cl bond, 2.340(1) Å which brings the possibility for replacement by the cyanido ligand. Two of three trans chromophore bond angles O1–Fe1–O2 and Cl1–Fe1–N2 are very close to linearity (176.93(9)° and 175.7(1)°, respectively); the third angle O–Fe–N is distorted significantly (163.7(1)°). Contrary to the other herein reported iron complexes with a similar type of pentadentate Schiff base ligands, the oxygen donor atoms are situated in the trans position.[45] The chlorine atom is involved in a weak hydrogen bond with the amino nitrogen atoms of the neighboring complex molecule (N2···Cl1, 3.433(3) Å), thus creating a 1D quasichain (see Supporting Information, Figure S5).

Single-crystal X-ray diffraction study of **2c** revealed a mononuclear Fe(III) complex with the deprotonated **1c** ligand (Figure 4), and four $[Fe(1c_{-2H})Cl]$ molecules are involved in the unit cell. The chromophore $\{FeO_2N_2N'Cl\}$ refers to a distorted octahedron. The Fe–N bond distances involving the imino bonds (2.091(2) and 2.103(2) Å) are shorter than that involving the amino nitrogen atom (2.199(2) Å). The Fe–O bond lengths are equal to 1.919(2) and 1.967(2) Å, and the Fe–Cl bond is much longer, 2.405(1) Å. Angles N–Fe–N and N2–Fe1–O1 significantly differ from linearity (161.23(9)° and 166.66(8)°). Due to the flexibility of the chlorido ligand, the deviation of the O2–Fe1–Cl1 angle is very small and the value

dx.doi.org/10.1021/ic3015833 | Inorg. Chem. 2012, 51, 12755–12767

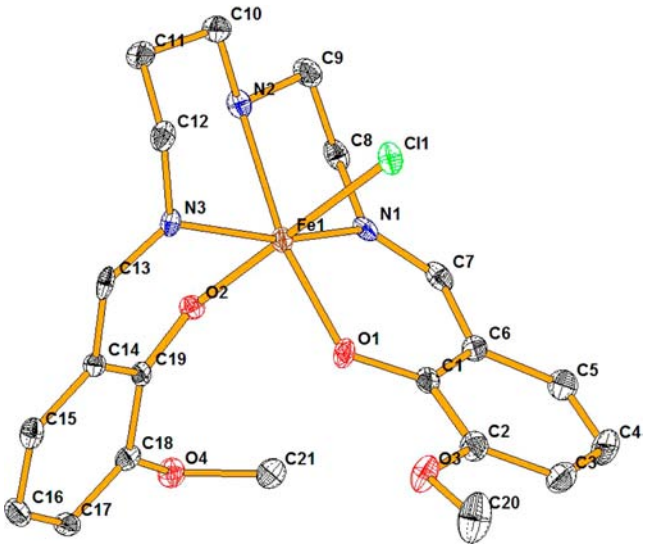

Figure 4. Crystal structure of mononuclear complex **2c** (50% probability level of thermal ellipsoids). Hydrogen atoms are omitted for clarity.

is very close to the flat angle (178.68(6)°). The oxygen donor atoms are in the cis arrangement and form an angle of 90.75(8)°. The chlorine atom creates intermolecular weak hydrogen bonds with the hydrogen atoms of the amino nitrogen atoms (N2···Cl1, 3.250(3) Å), thus creating a 1D quasichain (see Supporting Information, Figure S6).[44]

The asymmetric unit of **2d** consists of one complex molecule of formula [Fe(1a$_{-2H}$)NCS] and one molecule of methanol (Figure 5). Four [Fe(1a$_{-2H}$)NCS]·CH_3OH entities are

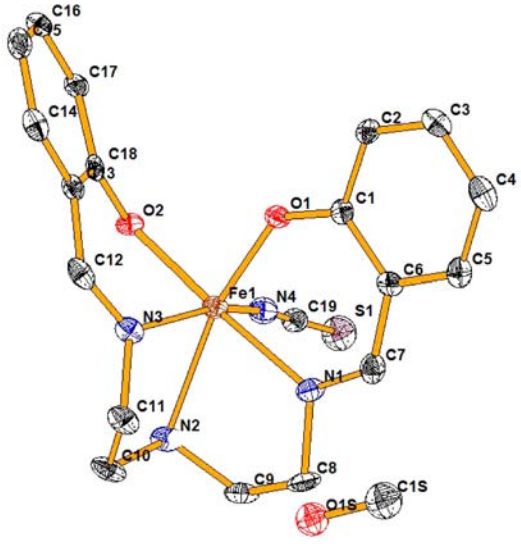

Figure 5. Molecular structure of mononuclear complex **2d** (50% probability level of thermal ellipsoids). Hydrogen atoms are omitted for clarity.

included in the unit cell. The bond lengths Fe−O (1.924(2) and 1.951(3) Å), Fe−N(thiocyanato) (2.061(3) Å), and two Fe−N(imino) show similar distances (2.151(4) and 2.236(3) Å), while the Fe−N(amino) is the longest one (2.236(3) Å). The angles between the central atom and the opposite donor atoms are significantly different from 180° (O1−Fe1−N2 = 159.4(1)°, N1−Fe1−O2 = 173.8(1)°, and O2−Fe1−N4 = 158.0(1)°), and they confirm that the {$FeN_2N'N''O_2$} chromophore forms a distorted octahedron. The oxygen donor atoms are positioned in the cis arrangement with the angle O−Fe−O = 89.5(1)°. The thiocyanato ligand is almost linear, and it is slightly bent with respect to the central atom (S1−N4−Fe1 = 173.06(5)°). A detailed inspection of the crystal structure reveals the existence of the supramolecular dimeric [Fe(1a$_{-2H}$)NCS]$_2$ structure created by hydrogen bonds between the phenolato oxygen and the amino nitrogen atoms (O2···N2, 2.882(3) Å, see Supporting Information, Figure S7) of the neighboring [Fe(1a$_{-2H}$)NCS] molecules and a weak hydrogen bond is present between thiocyanido sulfur and the oxygen atom from methanol (S1···OS1, 3.272(4) Å; see Supporting Information, Figure S7).[44]

Crystal Structures of Heptanuclear Compounds ***3a***, ***3b***, *and* ***3c***. Crystallographic data for the heptanuclear complexes are listed in Table 2. Single-crystal X-ray diffraction study of all three heptanuclear compounds confirmed the presence of the heptanuclear $[Fe^{II}(CN)_6\{Fe^{III}(1_{-2H})\}_6]^{2+}$ dications, two disordered chloride counteranions, and a few molecules of crystal water.

Heptanuclear Compound ***3a*** *[Fe(CN)$_6${Fe(1a$_{-2H}$)}$_6$]Cl$_2$·H$_2$O.* This compound contains one water molecule per complex unit, and four [Fe(CN)$_6${Fe(1a$_{-2H}$)}$_6$]Cl$_2$·H$_2$O entities are included in the unit cell. Diffraction data were collected at two temperatures (100 and 293 K) using the same crystal. For both measurements, the experiment revealed cubic *Pa*−3 symmetry. Thermal variation caused only negligible differences between the low- and the room-temperature structures. The inversion center of the heptanuclear dication is at the low-spin Fe(II) central atom, and the {FeC_6} chromophore refers to the regular octahedron with Fe1−C1 bond distances 1.915(47) Å at 100 K and 1.937(7) Å at room temperature.

Structural investigation of the complex cation {[Fe^{III}(1a$_{-2H}$)-NC]$_6$$Fe^{II}$}$^{2+}$ (Figure 6) revealed a unique coordination of the 1a$_{-2H}$ ligand moiety. Contrary to the so far published[24,26,34] or herein reported heptanuclear compounds, one ligand connects two Fe(III) centers (Figure 6, right). Such an exceptional coordination can be explained in two ways. It could be connected to an oligo- or a polymeric structure of **2a** mononuclear complex, where one 1a$_{-2H}$ ligand coordinates two Fe(III) central atoms in the same manner as in the structure of **3a**. Unfortunately, attempts to grow suitable single crystals of **2a** failed, but the high-resolution ESI ToF mass spectroscopy investigation of complex **2a** (see Supporting Information, Figure S4) revealed the presence of oligo/polymeric fragments (Supporting Information, Figure S4) and thus supports this idea. On the other hand, single-crystal X-ray analysis of **2d** with the same 1a$_{-2H}$ ligand moiety shows a standard coordination of one Schiff-base ligand to a single Fe(III) center. Therefore, the second possible explanation of the unusual structure of **3a** can be based on the kinetic lability of **2a**. Replacement of the chlorido for a cyanido group might cause a structural rearrangement of the donor atoms of the 1a$_{-2H}$ ligand moiety.

The centrosymmetry of the [Fe(CN)$_6${Fe(1a$_{-2H}$)}$_6$]$^{2+}$ cation is the reason for the structural equivalence of all six peripheral Fe(III) environments. The shape of the {$FeN_2N'N''O_2$} chromophore can be attributed to a distorted tetragonal bipyramid where the Fe−N bond lengths indicate the high-spin state at both temperatures of the experiment (Table 3). At 100 K, the bond lengths Fe−O are equal to 1.882(4) and 1.894(3) Å, respectively. The distances Fe−N(imino) are

dx.doi.org/10.1021/ic3015833 | *Inorg. Chem.* 2012, 51, 12755−12767

Table 2. Crystallographic Data for the Heptanuclear Complexes

	3a		3b	3c
formula	$C_{114}H_{116}Cl_2Fe_7N_{24}O_{13}$	$C_{114}H_{116}Cl_2Fe_7N_{24}O_{13}$	$C_{150}H_{229}Cl_2Fe_7N_{24}O_{44.50}$	$C_{132}H_{170}Cl_2Fe_7N_{24}O_{34}$
fw/g mol^{-1}	2492.16	2492.16	3540.37	3098.73
cryst color	black-violet	black-violet	black-violet	black-violet
temperature/K	100(2)	293(2)	100(2)	100(2)
wavelength/Å	0.71073	0.71073	1.54178	0.71073
cryst syst	cubic	cubic	monoclinic	trigonal
space group	*Pa*−3	*Pa*−3	$P2_1/c$	*R*−3
a/Å	23.934(3)	24.1809(7)	17.533(4)	29.4119(3)
b/Å	23.934(3)	24.1809(7)	16.893(3)	29.4119(3)
c/Å	23.934(3)	24.1809(7)	29.972(6)	15.4350(2)
α/deg	90	90	90.000(5)	90.00
β/deg	90	90	102.23(3)	90.00
γ/deg	90	90	90.000(5)	120.00
V/Å^3	13 710(3)	14 139.0(7)	8676(3)	11 563.3(2)
Z, ρ_{calcd}/g cm^{-3}	4, 1.207	4, 1.171	2, 1.356	3, 1.335
μ/mm^{-1}	0.819	0.794	5.528	0.752
F(000)	5152	5152	3738	4854
cryst size/mm	0.16 × 0.14 × 0.12	0.16 × 0.14 × 0.12	0.109 × 0.071 × 0.040	0.23 × 0.15 × 0.15
final *R* indices [$I > 2\sigma(I)$]	R_1 = 0.0325	R_1 = 0.0364	R_1= 0.0737	R_1 = 0.0426
	wR_2= 0.0864	wR_2= 0.1068	wR_2= 0.1691	wR_2= 0.1135
R indices (all data)	R_1= 0.0425	R_1 = 0.0466	R_1= 0.1200	R_1 = 0.0664
	wR_2 = 0.0891	wR_2 = 0.1100	wR_2 = 0.1806	wR_2 = 0.1180
GoF on F^2	1.078	1.105	1.001	1.047
CCDC ref. no.	838225	838226	838228	838227

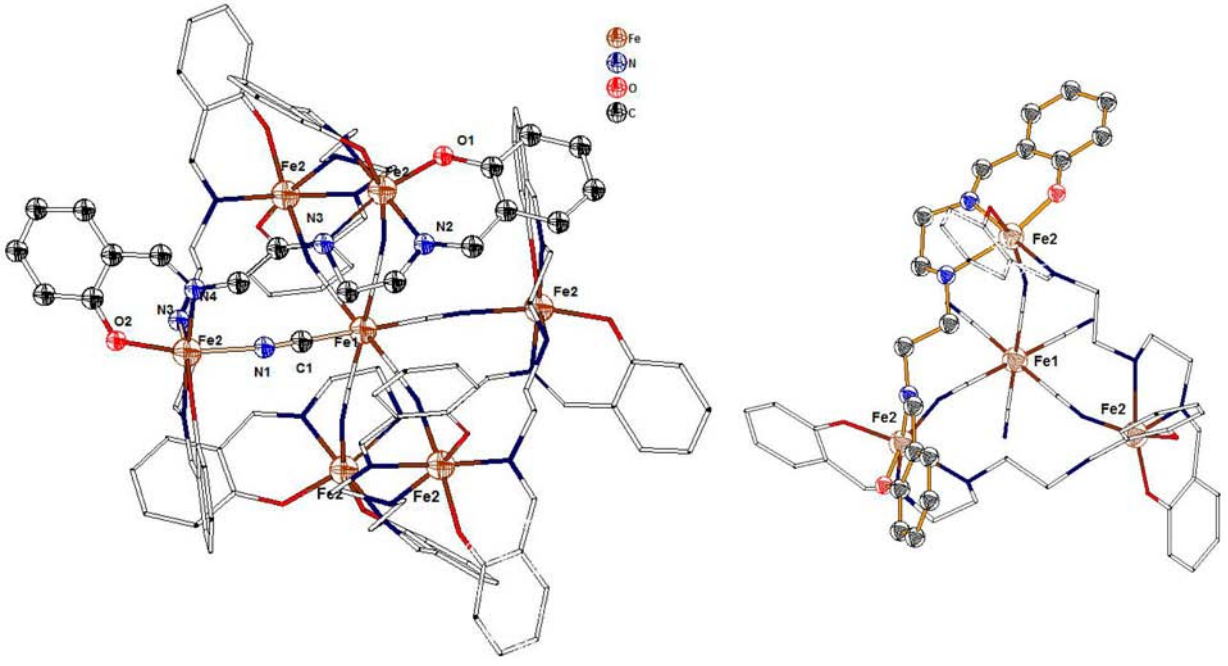

Figure 6. View of complex **3a**. (Left) Molecular structure of $[Fe(CN)_6\{Fe(1a_{-2H})\}_6]^{2+}$ complex. (Right) View of intramolecular ring in the crystal structure. Hydrogen atoms are omitted for clarity.

2.077(4) and 2.088(4) Å, and they are shorter than the Fe−N(amino) bond length which is 2.231(3) Å. The distance between the Fe^{III}−N(cyanido) is 2.079(4) Å, and it is close to that found in Prussian blue.[46]

Significant deviations from linearity are obvious for all three angles between the Fe(III) central atom and the trans-positioned donor atoms (N1−Fe2−N1 = 164.5(1)°, N1−Fe2−N2 = 176.5(2)°, N1−Fe2−N3 = 165.0(1)°). The oxygen donor atoms adopt the cis configuration, and they form the angle O−Fe−O = 97.0(1)°, which is a higher value than that found in the mononuclear complex **2d**. The Fe^{II}−C−N linkage is almost linear (177.9(4)°); however, the angle Fe^{III}−N−C exhibits a significant deviation from linearity (162.3(3)°).

The diffraction study of the compound **3b** was carried out at *T* = 100 K (Table 2). The compound crystallizes with 20.5 molecules of crystal water, and two $[Fe(CN)_6\{Fe(1b_{-2H})\}_6]$-$Cl_2$·20.5$H_2O$ entities can be found within the unit cell. The center of symmetry is represented by the diamagnetic Fe(II)

dx.doi.org/10.1021/ic3015833 | *Inorg. Chem.* 2012, 51, 12755−12767

Table 3. Selected Bond Lengths in the Heptanuclear Compounds[a]

	3a		3b			
			center Fe2	center Fe3	center Fe4	3c
$Fe^{III}–O_{(1)}$	1.882(4) [1.924(2)]	1.901(4)[b]	1.941(5) [1.957(3)]	1.933(4)	1.940(5)	1.922(2) [1.919(2)]
$Fe^{III}–O_{(2)}$	1.894(3) [1.951(3)]	1.922(4)[b]	1.994(4) [1.946(3)]	1.966(4)	1.976(5)	1.957(2) [1.967(2)]
$Fe^{III}–N(=C_1)$	2.077(4) [2.151(3)]	2.117(4)[b]	2.105(5) [2.104(4)]	2.119(6)	2.089(7)	2.085(2) [2.091(2)]
$Fe^{III}–N(=C_2)$	2.088(4) [2.090(3)]	2.108(4)[b]	2.127(5) [2.097(4)]	2.119(6)	2.118(7)	2.103(2) [2.103(2)]
$Fe^{III}–N(H)$	2.231(3) [2.236(3)]	2.266(3)[b]	2.228(6) [2.234(3)]	2.224(5)	2.242(5)	2.191(2) [2.199(2)]
$Fe^{III}–N(\equiv C)$	2.079(4)	2.110(4)[b]	2.042(6)	2.058(6)	2.026(7)	2.053(2)
$Fe^{II}–C(\equiv N)$	1.918(6)	1.937(7)[b]	1.922(8)	1.873(8)	1.927(9)	1.901(3)

[a]For comparison, bond lengths in related mononuclear complexes **2d**, **2b**, and **2c** are given in brackets. [b]Bond distances at 293 K.

central atom, coordinated by six cyanido ligands via the carbon atoms; the bond distances Fe–C vary in the range of 1.873–1.927 Å. Six peripheral Fe(III) centers are connected to the $[Fe(CN)_6]^{4-}$ building block through the nitrogen donor atoms of the cyanido bridge (Figure 7). Every $\{Fe^{III}(1b_{-2H})\}$ unit is

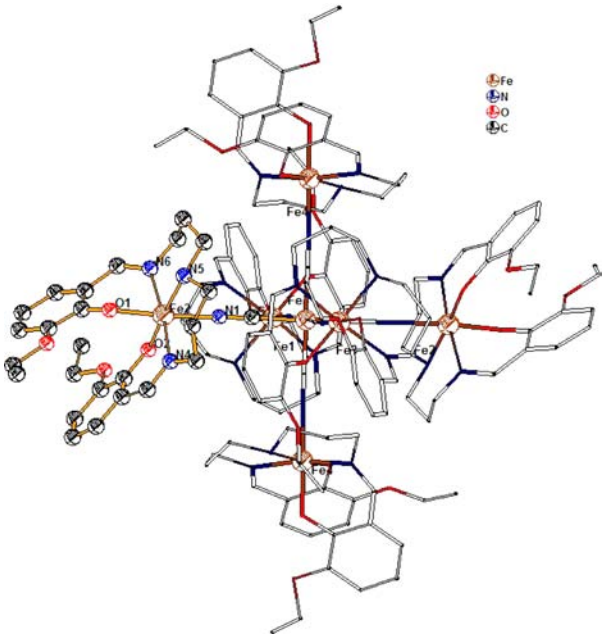

Figure 7. Molecular structure of the $[Fe(CN)_6\{Fe(1b_{-2H})\}_6]^{2+}$ cation in **3b**. Hydrogen atoms are omitted for clarity.

structurally equivalent with that in the trans position, and according to the bond lengths, the Fe(III) centers are high spin at T = 100 K (Table 3). Within the $\{FeN_2N'N''O_2\}$ chromophore the bond distances Fe–O span the range of 1.933(4)–1.994(4) Å, Fe–N(imine) vary as 2.089(7)–2.127(5) Å, and the longest bonds are Fe–N(amine) between 2.224(5) and 2.242(5) Å. The bond lengths Fe–N(cyanido) are 2.026(7)–2.058(6) Å; they are comparable to the related bonds in the crystal structure of Prussian blue.[46] The angles between the Fe(III) and the opposite donor atoms (three trans angles) are slightly diverted from linearity: the average value for O–Fe–N(amino) = 175.4°, N(amino)–Fe–N(amino) = 171.9°, and O–Fe–N(cyanido) = 176.0°. In comparison with the structure of the related complex **2b**, the oxygen donor atoms are rearranged to the cis configuration and form an average angle of O–Fe–O = 93.0°. The cyanido ligands coordinate to the very central Fe(II) atom in an almost linear manner: $Fe^{II}–C–N$ = 178.1° on average; on the other hand, the $C–N–Fe^{III}$ angles show a slight deviation from the flat angle (173.4° on average).

Single-crystal X-ray diffraction study of **3c** revealed that the compound contains the heptanuclear dication $[Fe(CN)_6\{Fe(1c_{-2H})\}_6]^{2+}$, 2 disordered Cl^- counteranions, and 10 molecules of crystal water (Table 2, Figure 8). The very

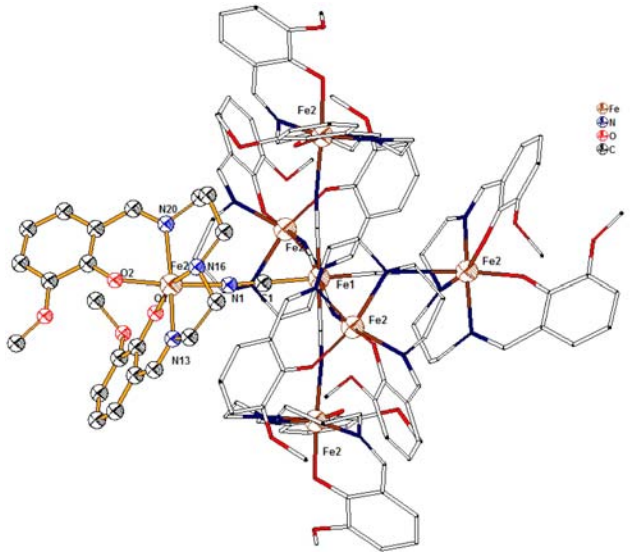

Figure 8. Molecular structure of the $[Fe(CN)_6\{Fe(1c_{-2H})\}_6]^{2+}$ cation in **3c**. Hydrogen atoms are omitted for clarity.

central Fe(II) atom represents an inversion center of the heptanuclear dication complex, and the chromophore $\{FeC_6\}$ refers to a perfect octahedron with bond lengths of 1.901(3) Å. The centrosymetric complex dication contains six peripheral structurally equivalent Fe(III) sites, and the bond lengths of the $\{Fe^{III}(1c_{-2H})\}$ coordination polyhedra indicate the high-spin state of Fe(III) at 100 K (Table 3). The shortest bonds are found for Fe–O (1.922(2)–1.957(2) Å); Fe^{III}–N(cyanido) bond lengths are comparable to those found in **3a**, **3b**, and Prussian blue;[46] the longest bonds are detected for Fe–N(amino) = 2.191(2) Å. The three trans angles are considerably declined from linearity: O1–Fe2–N16 = 165.2(2)°, N13–Fe2–N20 = 162.5(2)°, O2–Fe2–N1 = 174.6(2)°. The angle between the central atom and cis-positioned oxygen donor atoms is O1–Fe–O2 = 91.0(1)°. Also in this complex, the $Fe^{II}–C–N$ angle is very close to the flat angle (178.1°), but the $C–N–Fe^{III}$ angle is considerably bent and reaches 168.9°.

3.3. Magnetic Properties of Mononuclear Complexes.

The temperature variable magnetic investigation revealed a

dx.doi.org/10.1021/ic3015833 | Inorg. Chem. 2012, 51, 12755–12767

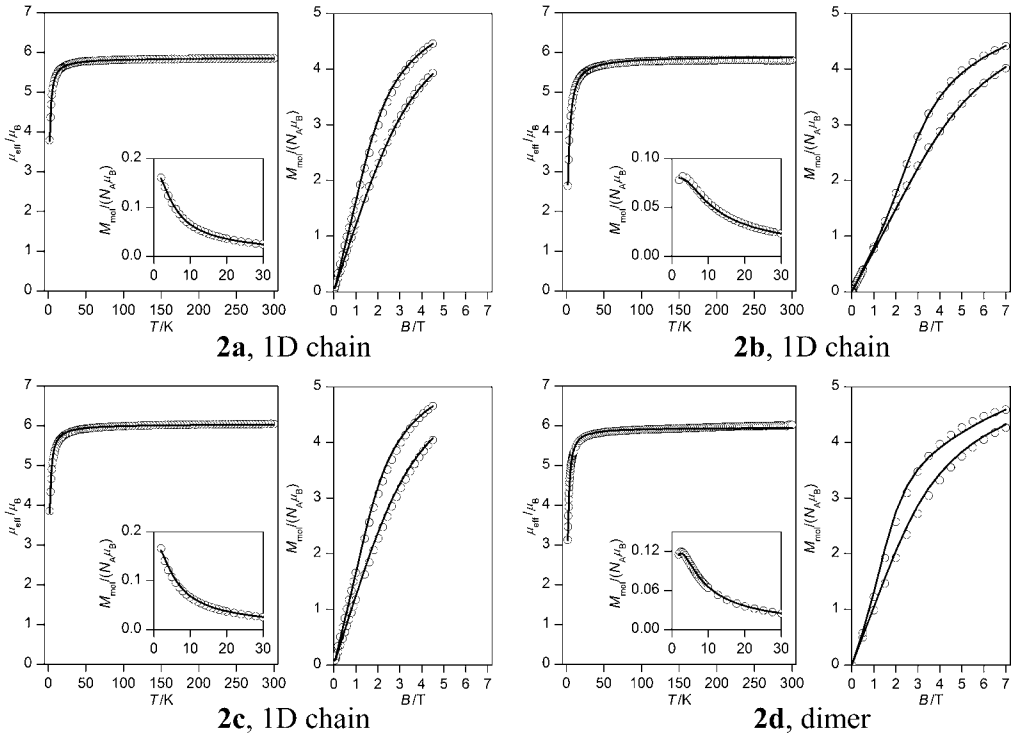

Figure 9. Temperature dependence of the effective magnetic moment (left) and molar magnetization (right) for **2a**−**d** scaled per monomer. (Inset) Molar magnetization measured at B = 0.1 T: (open symbols) experimental data, (lines) fitted according to eq 1 or 3.

high-spin paramagnetic behavior for all four mononuclear complexes, and in the temperature range of 300−50 K, the Currie law is obeyed (Figure 9). The effective magnetic moment μ_{eff} is constant in the temperature range of 50−300 K, and the room-temperature values of 5.85 for **2a**, 5.80 for **2b**, 6.04 for **2c**, and 6.02 for **2d** (in units of μ_B) are close to the spin-only value expected for the S = 5/2 system (5.92 μ_B). Below 50 K the μ_{eff} vs T curve adopts a decreasing character which is a fingerprint of the zero-field splitting and intermolecular interactions: μ_{eff} at 2 K falls to 3.79 for **2a**, 2.64 for **2b**, 3.85 for **2c**, and 3.13 for **2d** (in units of μ_B). Isothermal magnetizations were measured at T = 2 and 5 K up to B = 4.5 or 7 T, and experimental data corresponds to the S = 5/2 spin state affected by ZFS and/or weak antiferromagnetic interactions. Indeed, in the case of compounds **2b** and **2d**, the magnetic susceptibility passes through a rounded maximum which is a fingerprint of the exchange interactions of antiferromagnetic nature (J < 0). The maximum of the susceptibility for the [Fe^{III}···Fe^{III}] system is expected at T_{max} = $|J/k|$/0.347 when only the isotropic exchange applies.[42]

First, the magnetic properties of **2d** are discussed. It results from X-ray analysis that a quasidimer is formed through the N−H···O hydrogen bonds (see Supporting Information), and therefore, the following spin Hamiltonian was used in the magnetic data analysis

$$\hat{H}_a = -J(\vec{S}_1\cdot\vec{S}_2) + \sum_{A=1}^{2} D(\hat{S}_{A,z}^2 - \hat{S}_A^2/3) + \sum_{A}^{2} \mu_B B_a g \hat{S}_{A,a} \quad (1)$$

where = x and z. The first term stands for the isotropic exchange, the second term represents the zero-field splitting (D = an axial ZFS parameter), and the last contribution is the Zeeman term. As a result, 36 magnetic levels $\varepsilon_i = f(J, D, g, B_a)$ are used to calculate the partition function Z_a and subsequently the components of the molar magnetization

$$M_{mol,a} = N_A kT\left(\frac{\partial \ln Z_a}{\partial B_a}\right)_T \quad (2)$$

Then the magnetization of the powder sample is computed as an average over three Cartesian components: $M_{av} = (2M_x + M_z)/3$. The fitting procedure confirmed weak antiferromagnetic exchange (J < 0) together with positive D parameter; the final magnetic parameters are listed in Table 4.

Table 4. Magnetic Parameters for Mononuclear Complexes

	2a	2a	2b	2c	2d
model	dimer	1D chain	1D chain	1D chain	dimer
g	1.98	1.98	2.00	2.04	2.01
$(D/hc)/cm^{-1}$	+0.78	+0.68	+1.18	+0.61	+1.35
$(J/hc)/cm^{-1}$	−0.30	−0.18	−0.40	−0.20	−0.38

X-ray structures of **2b** and **2c** point to formation of quasi 1D chains, in both cases through the N−H···Cl hydrogen bonds (Supporting Information). Thus far, there are no analytical equations for 1D uniform chains with s = 5/2 including zero-field splitting. Therefore, we used the finite-size closed chain (ring) model with five centers

$$\hat{H}_a = -J[(\vec{S}_K\cdot\vec{S}_1) + \sum_{A=1}^{K-1}(\vec{S}_A\cdot\vec{S}_{A+1})] + \sum_{A=1}^{K} D(\hat{S}_{A,z}^2 - \hat{S}_A^2/3) + \sum_{A=1}^{K} \mu_B B_a g \hat{S}_{A,a} \quad (3)$$

The number of magnetic centers (K = 5) is supposed to be sufficient taking into account a very weak exchange as found in

dx.doi.org/10.1021/ic3015833 | Inorg. Chem. 2012, 51, 12755−12767

2d. Now, the number of magnetic energy levels is $(2s + 1)^5 = 7776$, and with the aim to speed up the computation, the symmetry-adapted basis set was generated using the spin permutational symmetry of the spin Hamiltonian[47] and D_5 point group of symmetry. Consequently, the whole interaction matrix is divided according to the irreducible representations to block A_1 ($N = 888$), A_2 ($N = 672$), E_1 ($N = 3\,108$), and E_2 ($N = 3\,108$). An analogous method has been recently applied to 1D Ni(II) chains.[48] The resulting energy levels were used to calculate molar magnetization similarly through the corresponding partition function. A simultaneous treatment of the temperature and field dependences of the molar magnetization again yielded a weak antiferromagnetic exchange and slight zero-field splitting, see Table 4.

For complex **2a** (the X-ray structure is undetermined) three models were tested: a monomer, dimer (see Supporting Information, Figure S8), and 1D chain; the last reconstructs the experimental data best. To conclude this part, thorough magnetic analysis revealed a weak antiferromagnetic exchange in the range from −0.18 to −0.40 cm^{-1} in compounds **2a**−**d** with positive zero-field splitting D parameter spanning the interval of 0.61−1.35 cm^{-1}.

3.4. Magnetic Properties of Heptanuclear Complexes.

The temperature variation of the effective magnetic moment for **3a**−**c** is shown in Figure 10. It can be seen that the overall

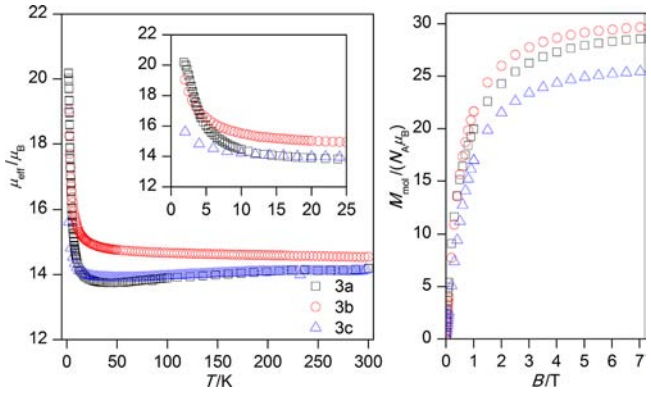

Figure 10. (Left) Temperature dependence of the effective magnetic moment for **3a** (squares), **3b** (circles), and **3c** (triangles). (Inset) Zoom of low-temperature data. (Right) Isothermal magnetization data measured at $T = 2$ K.

dependence is mutually similar; room-temperature data is close to the spin-only value expected for six uncoupled $s = 5/2$ centers: $\mu_{eff}/\mu_B = g[6s(s + 1)]^{1/2} = 14.5$. On cooling, sample **3b** exhibits a gradual increase of the effective magnetic moment that becomes rapid below 20 K. This behavior is a fingerprint of the overall ferromagnetic exchange. The inverse susceptibility is nearly linear, and it extrapolates to a zero value at slightly positive temperature ($\Theta > 0$).

Herein, we studied the magnetic properties of **3b** in more detail. First, the purely isotropic model was used taking into account that the paramagnetic iron(III) centers are interconnected through diamagnetic hexacyanidoferrate(II). Therefore, the following spin Hamiltonian including the isotropic exchange and the Zeeman term was postulated to interpret magnetic properties ($N = 6$)

$$\hat{H} = -\sum_{A=1}^{N}\sum_{B<A}^{N} J(\vec{S}_A\cdot\vec{S}_B) + \sum_{A=1}^{N} \mu_B B_z g \hat{S}_{A,z} \quad (4)$$

The advantage of this Hamiltonian is that an analytical expression for energy levels is available in the coupled basis set

$$\varepsilon(S, M_S) = -JS(S + 1)/2 + \mu_B B g M_S \quad (5)$$

where S is the final spin state and M_S its projection. The individual spin states $S = 0, 1, ..., 15$ occur $d_S = 111, 315, 475, 575, 609, 581, 505, 405, 300, 204, 126, 70, 35, 15, 5$, and 1 times. Now, all 46 656 magnetic energy levels are used to calculate the molar magnetization

$$M_{mol} = N_A\mu_B g \frac{\sum_{S=0}^{15}\sum_{M_S=-S}^{+S} d_S M_S \exp[-\varepsilon(S, M_S)/kT]}{\sum_{S=0}^{15}\sum_{M_S=-S}^{+S} d_S \exp[-\varepsilon(S, M_S)/kT]} \quad (6)$$

The fitting procedure resulted in $(J/hc) = +0.057$ cm^{-1} and $g = 2.01$, thus confirming the weak ferromagnetic exchange present in **3b**. The reconstructed data are displayed in Figure 11 (gray

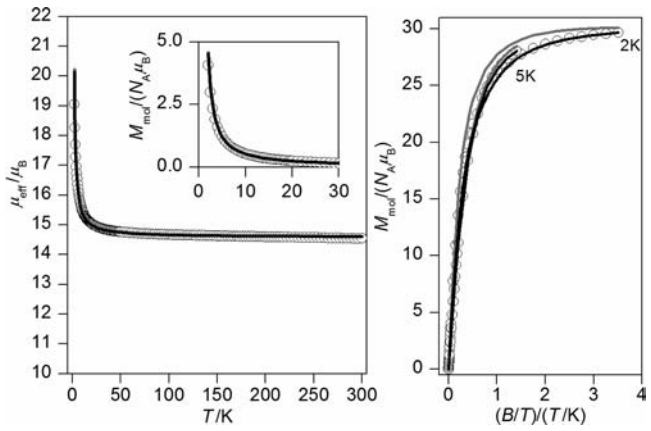

Figure 11. Temperature dependence of the effective magnetic moment (left) and molar magnetization (right) for **3b**. (Inset) Molar magnetization measured at $B = 0.1$ T: (open symbols) experimental data, (gray lines) fitted according to eq 4, (black line) fitted according to eq 7.

lines). The experimental reduced magnetization data $M_{mol} = f(B/T)$ for two temperatures do not coincide; thus, we can suppose that also the magnetic anisotropy plays an important role in this compound, as demonstrated for **2a** and **2b**.

Therefore, the spin Hamiltonian was enriched by the single-ion zero-field splitting term as follows

$$\hat{H} = -\sum_{A=1}^{N}\sum_{B<A}^{N} J(\vec{S}_A\cdot\vec{S}_B) + \sum_{A=1}^{N} D(\hat{S}_{A,z}^2 - \hat{S}_A^2/3) + \sum_{A=1}^{N} \mu_B B_a g \hat{S}_{A,a} \quad (7)$$

Unfortunately, there is no analytical formula for energy levels, and all 46 656 magnetic levels must be treated numerically. In order to make this calculation feasible, the symmetry-adapted local basis set was generated using spin permutational symmetry of the spin Hamiltonian[47] and D_6 point group of symmetry. Consequently, the whole interaction matrix is divided according to the irreducible representations to blocks A_1 ($N = 4291$), A_2 ($N = 3535$), B_1 ($N = 4145$), B_2 ($N = 3605$), E_1 ($N = 15\,470$), and E_2 ($N = 15\,610$). Subsequently, magnetization was calculated using eq 2, and the fitting procedure resulted in $(J/hc) = +0.052$ cm^{-1}, $(D/hc) = +0.49$

dx.doi.org/10.1021/ic3015833 | Inorg. Chem. 2012, 51, 12755−12767

cm^{-1}, and g = 2.01 (Figure 11, black lines). The D parameter has a similar value to the herein reported mononuclear precursors **2a** and **2b**, and very good agreement was found between experimental and calculated isothermal magnetizations.

Samples **3a** and **3c** show slightly different behavior in comparison with **3b**. First, there is a small decrease of the effective magnetic moment on cooling from room temperature, and then below 50 K a rapid increase occurs. This suggests that dominant ferromagnetic interactions are prevailing; however, also other phenomena must be present as the saturation value of $M_{mol}/N_A\mu_B$ at 2 K is significantly reduced in contrast with the theoretical value of $M_{mol}/N_A\mu_B$ = 30 for S_{max} = 30/2. We found that this behavior was observed for several independently prepared batches of **3a** and **3c**, so it seems to us that it is an intrinsic property of these two compounds. To rationalize this behavior, several hypotheses were tested.

First, the phase purity of investigated samples was tested before magnetic investigation, so the presence of various polymorphic forms with a different number of lattice solvent molecules can be ruled out (Figure S9, Supporting Information). The second hypothesis is that subtle changes in the structure of **3a** and **3c** (the $\{Fe^{II}C_6\}$ chromophore in complexes **3a** and **3c** is octahedral; in **3b** is rhombohedral) may result in competition of ferromagnetic and antiferromagnetic interaction among Fe(III) centers through diamagnetic ferrocyanide (Figure S10, Supporting Information). However, this model is not capable to explain the temperature dependence of μ_{eff}/μ_B and reduced saturation limit of the isothermal magnetization.

Another presumption is that a minor amount of iron(III) central atoms undergo a gradual spin cross-over phenomenon analogously, e.g., to $[Cr\{(CN)Fe(^5L)\}_3(CN)_3]$ ($^5LH_2$ = *N*,*N*′-bis(1-hydroxy-2-benzylidene)-1,7-diamino-4-azaheptane).[33] This would explain the decrease of μ_{eff}/μ_B on cooling with subsequent increase of the effective magnetic moment due to ferromagnetic interaction in heptanuclear complexes and also reduction of the saturation limit of magnetization. For instance, a combination of 5 × Fe (HS, S = 5/2, g = 2.0) and 1 × Fe (LS, S = 1/2, g = 2.2) would result in a decrease of μ_{eff}/μ_B from 14.5 to 13.4, and $M_{mol}/N_A\mu_B$ would saturate to 26.1.

The last assumption is that a spin admixing is taking place. Spin-admixed states were observed in tetra-,[49] penta-,[50] and also hexacoordinated[51] iron(III) complexes. In reported complexes, the peripheral Fe(III) centers are far from the octahedral environment owing to the different nature and lengths of Fe−O and Fe−N bonds, respectively. As the local excited state $^4A_2$ for a distorted hexacoordinate Fe(III) system is close to the ground state $^6A_1$, it is legitimate to deal with the spin-admixed states $\{^6A_1,^4A_2\}$.[42,52,53] Such interaction would lead to mixing of S = 5/2 and 3/2 states resulting in lowering the effective magnetic moment and also the saturation limit of the isothermal magnetization ($M_{mol}/N_A\mu_B$ = 28 and 25 for **3a** and **3c**, respectively). Accepting these data as the saturation values, the percentage of the intermediate s = 3/2 state is readily calculated as P = 7 and 15% (g = 2 is assumed). Despite the fact that a simplified model for spin-admixed states, the so-called Maltempo model,[54,55] exists, it is beyond the scope of this work to extend such model to six interacting Fe(III) centers (the model space is spanned by $N = 10^6$ spin−orbital functions). As a result, we leave these last two hypotheses as a possible explanation of peculiar magnetic behavior of compounds **3a** and **3c**.

3.5. Mössbauer Spectroscopy. The transmission ^{57}Fe Mössbauer spectra for compounds **2a**, **3a**, and **3b** were collected at room temperature, and in the case of **2a** and **3b** also the low-temperature spectra were acquired. Analysis of the experiments for mononuclear complex **2a** revealed single-component spectra with parameters typical for the high-spin Fe(III) coordination center at both temperatures, Table 5. The isomer shift decreases on increasing temperature, which can be attributed to the second-order Doppler effect,[56] and also the reduction of quadrupole splitting upon heating is observed. In the case of the heptanuclear mixed-valence complex **3a**, the room-temperature spectrum consists of two doublets: the dominant one is assigned to the high-spin Fe(III) centers and the minor one corresponds to the low-spin Fe(II) center. The former one has similar properties (δ and ΔE_Q) as in the mononuclear compound **2a**. Similar features were observed for the spectra of **3b** taken at 300 K (Figure 12). Upon cooling the sample to 25 K, the increase of the isomer shift and quadrupole splitting is detected, which is in accordance with the temperature dependence of the Mösssbauer spectra of **2a** (Table 5). The area ratio between two components of **3b** at 25 K is 85:15, which is in excellent agreement with the expected value of 86:14 for the 6:1 ratio of the Fe(III)/Fe(II) ions in the heptanuclear complex. However, the area ratio is changed at 300 K to 77:23 for **3b** and 79:21 for **3a**, which might be caused by the different temperature dependence of Debye−Waller factors for the high-spin Fe(III) and low-spin Fe(II) centers.[57−59]

Table 5. Mössbauer Spectra Parameters for Complexes 2a and 3b[a]

compound	T/K	δ/mm s^{-1}	ΔE_Q/mm s^{-1}	A/%	site assignment
2a	25	+0.37	0.63	100	Fe^{III} HS
	300	+0.26	0.59	100	Fe^{III} HS
3a	300	+0.28	0.64	79	Fe^{III} HS
		−0.26	0.14	21	Fe^{II} LS
3b	300	+0.38	0.82	77	Fe^{III} HS
		−0.14	0.00	23	Fe^{II} LS
	25	+0.47	0.97	85	Fe^{III} HS
		−0.04	0.20	15	Fe^{II} LS

[a]Four parameters refer to each deconvolution line: quadrupole splitting Q_i, isomer shift δ_i, height, and width of the Lorenzian line; the parameter set is enlarged by a baseline. The area A_i for individual quadrupole doublets has been evaluated by a numerical integration

4. CONCLUSIONS

Three new Prussian blue analogues—the heptanuclear mixed-valence iron complexes **3a**, **3b**, and **3c** of the $[Fe^{II}(CN)_6\{Fe^{III}1_{-2H}\}_6]Cl_2{\cdot}nH_2O$ general formula (**3a** with n = 1, **3b** with n = 20.5, and **3c** with n = 10)—were synthesized and structurally and spectrally characterized, and their magnetic properties were investigated in detail. Preparation of the heptanuclear complexes consists of three steps. In the first, the free pentadentate ligands **1a**, **1b**, and **1c** were prepared by Schiff condensation between the derivatives of salicylaldehydes and various aliphatic triamines. In the next step, the "in situ" prepared ligands were reacted with the Fe(III) central ions and three mononuclear complexes **2a**, **2b**, and **2c** of general formula $[Fe(1_{-2H})Cl]$ were formed (1_{-2H} are doubly deprotoned forms of the Schiff base ligand **1**). In the final part, the mononuclear $[Fe(1_{-2H})Cl]$ precursors are clustered on the $[Fe(CN)_6]^{4-}$

dx.doi.org/10.1021/ic3015833 | Inorg. Chem. 2012, 51, 12755−12767

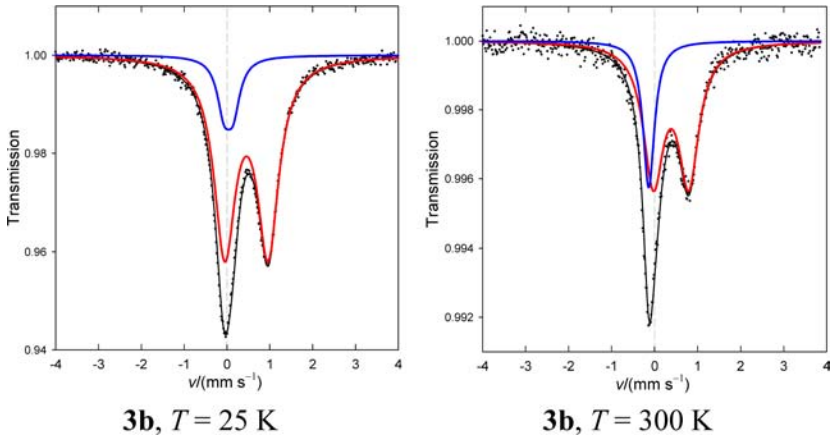

Figure 12. Mössbauer spectra for heptanuclear complex **3b**.

bridging anion, which rises into formation of the heptanuclear mixed-valence complexes. Also, a mononuclear complex **2d** of formula [Fe(1_{-2H})NCS] was prepared for a comparative study with **2a** and **3a**.

Structural study of the mononuclear complexes showed coordination of one pentadentate N_3O_2 Schiff-base ligand to a single Fe(III) central atom, and the sixth coordination site is occupied by the chlorido and/or thiocyanato ligand. Two oxygen donor atoms of the ligand moiety can coordinate the Fe(III) atom either in the cis or in the trans configuration. A detailed look into the crystal structures revealed the presence of intermolecular connectivity via hydrogen bonds. Magnetometry confirms that all mononuclear Fe(III) complexes exist in the high-spin state. Short Fe···Fe contacts were identified in the crystal structure of **2b**, **2c**, and **2d**; these rationalize the presence of weak magnetic exchange interactions. The magnetic data (temperature and field dependence of the magnetization) were fitted to a dimeric model for **2d** and a 1D chain model for **2b** and **2c**. For **2a** both models were investigated (the monomeric model gave unsatisfactory results). The exchange interaction is weak-negative, whereas the axial zero-field spitting is weak-positive.

The crystal structures of **3a**, **3b**, and **3c** contain a heptanuclear complex dication which consists of the ferrocyanide core whose octahedral nodes are coordinated by six peripheral {Fe(1_{-2H})} units. Compound **3a** shows an unusual type of coordination, where one pentadentate ligand moiety interconnects two neighboring Fe(III) centers and forms intramolecular rings. Complexes **3b** and **3c** exhibit usual coordination modes with one pentadentate ligand capping one Fe(III) central atom. Magnetic investigation of heptanuclear complexes also revealed the high-spin state of all six Fe(III) coordination sites ($s = 5/2$), whereas the very central Fe(II) site is in the low-spin state ($s = 0$). At low temperature, the ferromagnetic exchange interactions stay evident owing to which the ground state is $S = 15$ (30 unpaired electrons) for all three cases. Furthermore, the advanced theoretical treatment, including single-ion axial zero-field splitting parameter D_{Fe} for all six Fe(III) ions, was found necessary for proper description of the experimental magnetic data. Direct comparison of D in mononuclear precursor **2b** ($D_{Fe} = +1.18$ cm^{-1}) and final heptanuclear compound **3b** ($D_{Fe} = +0.49$ cm^{-1}) reveals information about the change of the magnetic anisotropy upon coordination of building blocks into more complex structures, information which is important for the class of single-molecule magnets and the height of their energy barrier for spin reversal. The magnetic behavior of **3a** and **3c** is very similar and slightly differs from **3b**. We assume that besides the dominant ferromagnetic interaction, the unusual minimum in the μ_{eff} vs T curve indicates the presence of either gradual and incomplete spin transition or spin-admixing effect. Mössbauer spectroscopy of the mononuclear complex **2a** confirmed the high-spin state of the Fe(III) central atom which is in agreement with the magnetic data. For heptanuclear complexes **3a** and **3b** it revealed the presence of two different doublets for both compounds. The first major doublet is related to six Fe(III) high-spin coordination sides and the second minor doublet refers to the low-spin very central Fe(II).

Only two reports of X-ray structural data have been reported for a compound analogous to **3a**, **3b**, and **3c** so far,[24,26,35] so that the present study enriches the structural and magnetic data for this class of star-like high-spin molecular compounds.

■ ASSOCIATED CONTENT

Ⓢ Supporting Information

Details of the infrared and ESI ToF spectra and structural and magnetic information. The cif files for the reported structure can be retrieved from the Cambridge Crystallographic Data center. This material is available free of charge via the Internet at http://pubs.acs.org.

■ AUTHOR INFORMATION

Corresponding Author

*E-mail: ivan.salitros@stuba.sk.

Notes

The authors declare no competing financial interest.

■ ACKNOWLEDGMENTS

Grant Agencies (Slovakia: VEGA 1/0052/11, APVV-0014-11, and APVV-0132-11; Czech Republic: GAČR P207/11/0841 and KAN115600801; Germany: DAAD-DE/SK), the Operational Program Research and Development for Innovations—European Regional Development Fund (CZ.1.05/2.1.00/03.0058), and the Operational Program Education for Competitiveness—European Social Fund (CZ.1.07/2.3.00/20.0017) of the Ministry of Education, Youth and Sports of the Czech Republic are acknowledged for financial support. Prof. Radek Zbořil (Palacky University, Olomouc, Czech Republic) and Dr. M. Klein (Leibniz University, Hannover, Germany) are greatly appreciated for performing Mössbauer

spectra of reported compounds. Dr. A. Eichhoefer (Karlsruhe Institute of Technology, Germany) and Tibor Dubai are greatly appreciated for performing XRPD spectra and TG/DTA analysis of reported compounds.

REFERENCES

(1) Rebilly, J. N.; Mallah, T. *Struct. Bonding (Berlin)* **2006**, *122*, 103.
(2) Culp, J. T.; Park, J. H.; Frye, F.; Huh, Y. D.; Meisel, M. W.; Talham, D. R. *Coord. Chem. Rev.* **2005**, *249*, 2642.
(3) Guennic, B.; Borshch, S.; Robert, V. *Inorg. Chem.* **2007**, *46*, 11106.
(4) Sato, O. *Acc. Chem. Res.* **2003**, *36*, 692.
(5) Papanikolaou, D.; Margadonna, S.; Kosaka, W.; Ohkoshi, S.; Brunelli, M.; Prassides, K. *J. Am. Chem. Soc.* **2006**, *128*, 8358.
(6) Li, D.; Clérac, R.; Roubeau, O.; Harté, E.; Mathoniere, C.; Le Bris, R; Holmes, S. M. *J. Am. Chem. Soc.* **2008**, *130*, 252.
(7) Ohkoshi, S.; Tokoro, H.; Hashimoto, K. *Coord. Chem. Rev.* **2005**, *249*, 1830.
(8) Itaya, K.; Uchida, I.; Neff, V. *Acc. Chem. Res.* **1986**, *19*, 162.
(9) Sato, O.; Gu, Z.; Etoh, H.; Ichiyanagi, J.; Iyoda, T.; Fujishima, A.; Hashimoto, K. *Chem. Lett.* **1997**, 37.
(10) Sato, O.; Einaga, Y.; Iyoda, T.; Fujishima, A.; Hashimoto, K. *J. Electrochem. Soc.* **1997**, *144*, L11.
(11) Karyakin, A. A. *Electroanalysis* **2001**, *13*, 813.
(12) Ferlay, S.; Mallah, T.; Ouahès, R.; Veillet, P.; Verdaguer, M. *Nature* **1995**, *378*, 701.
(13) Entley, W. R.; Girolami, G. S. *Science* **1995**, *268*, 397.
(14) Holmes, S. M.; Girolami, G. S. *J. Am. Chem. Soc.* **1999**, *121*, 5593.
(15) Hagen, K. S.; Naik, S. G.; Huynh, B. H.; Masello, A.; Christou, G. *J. Am. Chem. Soc.* **2009**, *131*, 7516.
(16) Garde, R; Villain, F.; Verdaguer, M. *J. Am. Chem. Soc.* **2002**, *124*, 10531.
(17) Fukita, N.; Ohba, M.; Okawa, H.; Matsuda, K.; Iwamura, H. *Inorg. Chem.* **1998**, *37*, 842.
(18) Ohba, M.; Usuki, N.; Fukita, N.; Okawa, H. *Angew. Chem., Int. Ed.* **1999**, *38*, 1795.
(19) El Fallah, M. S.; Rentschler, E.; Caneschi, A.; Sessoli, R.; Gatteschi, D. *Angew. Chem., Int. Ed.* **1996**, *35*, 1947.
(20) Ohba, M.; Maruono, N.; Okawa, H.; Enoki, T.; Latour, J. M. *J. Am. Chem. Soc.* **1994**, *116*, 11566.
(21) Miyasaka, H.; Okawa, H.; Miyazaki, A.; Enoki, T. *Inorg. Chem.* **1998**, *37*, 4878.
(22) Ohba, M.; Usuki, N.; Fukita, N.; Okawa, H. *Inorg. Chem.* **1998**, *37*, 3349.
(23) Mallah, T.; Auberger, C.; Verdaguer, M.; Veillet., P. *J. Chem. Soc., Chem. Commun.* **1995**, 61.
(24) Parker, R. J.; Hockless, D. C.R.; Moubaraki, B.; Murray, K. S.; Spiccia, L. *Chem. Commun.* **1996**, 2789.
(25) Rogez, G.; Marvilliers, A.; Riviére, E.; Audiére, J. P.; Lloret, F.; Varret, F.; Goujon, A.; Mendenez, N.; Girerd, J. J.; Mallah, T. *Angew. Chem., Int. Ed.* **2000**, *39*, 2885.
(26) Rogez, G.; Parsons, S.; Paulsen, C.; Villar, V.; Mallah, T. *Inorg. Chem.* **2001**, *40*, 3836.
(27) Gembický, M.; Boča, R.; Renz, F. *Inorg. Chem. Commun.* **2000**, *3*, 662.
(28) Boča, R.; Šalitroš, I. *Chem. Pap.* **2008**, *62*, 575.
(29) Glaser, T.; Heidemeier, M.; Weyhermüller, T.; Hoffmann, R. D.; Rupp, H.; Müller, P. *Angew. Chem., Int. Ed.* **2006**, *45*, 6033.
(30) Miyasaka, H.; Matsumoto, N.; Okawa, H.; Re, N.; Gallo, E.; Floriani, C. *J. Am. Chem. Soc.* **1996**, *118*, 981.
(31) Ni, W. W.; Ni, Z. H.; Cui, A. L.; Liang, X.; Kou, H. Z. *Inorg. Chem.* **2007**, *46*, 22.
(32) Re, N.; Gallo, E.; Floriani, C.; Miyasaka, H.; Matsumoto, N. *Inorg. Chem.* **1996**, *35*, 6004.
(33) Herchel, R.; Boča, R.; Gembický, M.; Kožíšek, J.; Renz, F. *Inorg. Chem.* **2004**, *43*, 4103.
(34) Šalitroš, I.; Boča, R.; Dlháň, L′.; Gembický, M.; Kožíšek, J.; Linares, J.; Moncol′, J.; Nemec, I.; Perašínová, L.; Renz, F.; Svoboda, I.; Fuess, H. *Eur. J. Inorg. Chem.* **2009**, 3141.
(35) Boča, R.; Šalitroš, I.; Kožíšek, J.; Linares, J.; Moncol′, J.; Renz, F. *Dalton Trans.* **2010**, *39*, 2198.
(36) Clark, R. C.; Reid, J. S. *Acta Crystallogr.* **1995**, *A51*, 887.
(37) Oxford Diffraction. *CrysAlis CCD and CrysAlis RED*; Oxford Diffraction Ltd.: Abingdon, England, 2006.
(38) Sheldrick, G. M. *Acta Crystallogr.* **2008**, *A64*, 112.
(39) Altomare, A.; Burla, M. C.; Camalli, M.; Cascarano, G. L.; Giacovazzo, C.; Guagliardi, A.; Moliterni, A. G. G.; Polidori, G.; Spagna, R. *J. Appl. Crystallogr.* **1999**, *32*, 115.
(40) Van der Sluis, P.; Spek, A. L. *Acta Crystallogr.* **1990**, *A46*, 194.
(41) Spek, A. L. *J. Appl. Crystallogr.* **2003**, *36*, 7.
(42) Boča, R. *Theoretical Foundations of Molecular Magnetism*; Elsevier: Amsterdam, 1999.
(43) Gaber, B. P.; Miskowski, V.; Spiroc, T. G. *J. Am. Chem. Soc.* **1974**, *96*, 6868.
(44) Desiraju, G. R.; Steiner, T. *The weak hydrogen bond*; IUCr Oxford Science Publication: New York, 1999.
(45) Nemec, I.; Boča, R.; Gembický, M.; Dlháň, L.; Herchel, R.; Renz, F. *Inorg. Chim. Acta* **2009**, *362*, 4754.
(46) Buser, H. J.; Schwarzenbach, D.; Petter, W.; Ludi, A. *Inorg. Chem.* **1977**, *16*, 2704.
(47) Waldmann, O. *Phys. Rev. B: Condens. Matter Mater. Phys.* **2000**, *61*, 6138.
(48) Nemec, I.; Herchel, R.; Boča, R.; Svoboda, I.; Trávníček, Z.; Dlháň, L.; Matelková, K.; Fuess, H. *Inorg. Chim. Acta* **2011**, *366*, 366.
(49) Alonso, P. J.; Arauzo, A. B.; Forniés, J.; García-Monforte, M. A.; Martín, A.; Martínez, J. I.; Menjón, B.; Rillo, C. JJ.; Sáiz-Garitaonandia, J. J. *Angew. Chem., Int. Ed.* **2006**, *45*, 6707.
(50) Weiss, R.; Gold, A.; Terner., J. *Chem. Rev.* **2006**, 2550.
(51) Kintnert, E. T.; Dawson, J. H. *Inorg. Chem.* **1991**, *30*, 4892.
(52) Boča, R. *A Handbook of Magnetochemical Formulae*; Elsevier: Amsterdam, 2012.
(53) Kahn, O. *Molecular Magnetism*; VCH: New York, 1993.
(54) Maltempo, M. M. *J. Chem. Phys.* **1974**, *61*, 2540.
(55) Maltempo, M. M.; Moss, T. H.; Cusanovich, M. A. *Biochim. Biophys. Acta* **1974**, *342*, 290.
(56) Greenwood, N. N.; Gibb, T. C. *Mössbauer Spectroscopy*; Chapman and Hall Ltd.: London, 1971.
(57) Eynatten., G.; Bommel, H. E. *Appl. Phys.* **1997**, *14*, 415.
(58) Real, J. A.; Bolvin, H.; Bousseksou, A.; Dworkin, A.; Kahn, O.; Varret, F.; Zarembowitch, J. *J. Am. Chem. Soc.* **1992**, *114*, 4650.
(59) Rabah, H.; Guillin, J.; Cereze-Ducouret, A.; Greneche, J.-M.; Talham, D; Boukheddaden, K.; Linares, J.; Varret, F. *Hyperfine Interact.* **1993**, *77*, 51.